

Critical point of nuclear matter and beam-energy dependence of net-proton number fluctuations

Volodymyr Vovchenko,^{1,2} Lijia Jiang,² Mark I. Gorenstein,^{2,3} and Horst Stoecker^{1,2,4}

¹*Institut für Theoretische Physik, Goethe Universität Frankfurt, D-60438, Frankfurt am Main, Germany*

²*Frankfurt Institute for Advanced Studies, Giersch Science Center, D-60438, Frankfurt am Main, Germany*

³*Bogolyubov Institute for Theoretical Physics, 03680 Kiev, Ukraine*

⁴*GSI Helmholtzzentrum für Schwerionenforschung GmbH, D-64291 Darmstadt, Germany*



(Received 28 November 2017; revised manuscript received 28 February 2018; published 15 August 2018)

The beam energy dependence of net baryon number susceptibilities is studied in the framework of the hadron resonance gas model with the attractive and repulsive van der Waals interactions between baryons. The collision energy dependences for the skewness $S\sigma$ and kurtosis $\kappa\sigma^2$ deviate significantly from the Poisson baseline and demonstrate the existence of rich structures at moderate collision energies. This behavior may result from the critical end point of the nuclear liquid-gas first-order phase transition. In particular, $\kappa\sigma^2$ shows a nonmonotonic energy dependence, and, in contrast to the standard scenario for the QCD critical point, it does not decrease at low collision energies. It is also found that the measurable net proton fluctuations differ significantly from the net baryon fluctuations when interactions between baryons cannot be neglected. The results are compared with the experimental net proton number fluctuations measured by the STAR collaboration.

DOI: [10.1103/PhysRevC.98.024910](https://doi.org/10.1103/PhysRevC.98.024910)

I. INTRODUCTION

One of the main goals of today's experiments in nucleus-nucleus ($A + A$) collisions is to search for the critical point (CP) of QCD matter [1–5] (see also recent reviews [6,7]). Theoretical arguments suggest the enhancement of net baryon number fluctuations in the critical region [1,2,8–11]. On the experimental side, the STAR collaboration has presented the beam energy scan data of proton cumulants in Au+Au collisions for center of mass energies per nucleon pair, $\sqrt{s_{NN}}$, of the BNL Relativistic Heavy Ion Collider (RHIC) from 7.7 GeV to 200 GeV. At moderate collision energies, the data [12–14] on skewness $S\sigma$ and kurtosis $\kappa\sigma^2$ of the net proton number fluctuations show an interesting nonmonotonic behavior and exhibit large deviations from the Poisson baseline. This is considered as a possible signal for the CP [15–21]. The experimental data are also influenced by other effects, such as initial state fluctuations [22], system volume fluctuations [23–25], stopping effects [26], acceptance effects [27,28], global charge conservation [29,30], effects of the hadronic phase [11,31], etc. Some of these effects have been studied with transport models [32–34]. It has also been argued that correlation functions, expressible through cumulants, may provide cleaner information about the underlying dynamics in heavy-ion collisions [35].

In this paper, we focus on the interactions between baryons within the quantum van der Waals (QvdW) equation of state [36–38]. In Ref. [39] the hadron resonance gas (HRG) model with QvdW interactions between baryons and between antibaryons was formulated and compared with lattice QCD simulations at zero chemical potentials in the crossover temperature region. Inclusion of the QvdW interactions has only a minor influence on the pressure and energy density in comparison with the ideal HRG (IHRG) model, but they

change significantly the structure of all high-order fluctuations of conserved charges, in most cases leading to a much better agreement with the lattice data, e.g., a quantitative agreement up to $T \simeq 160$ MeV is obtained for the net baryon number susceptibilities. The influence of nucleon-nucleon interactions and the associated nuclear liquid-gas criticality on baryon number fluctuations had previously also been pointed out in Refs. [40,41]. In the following, we calculate the baryon number fluctuations along the chemical freeze-out line within the QvdW-HRG model and make a comparison with the STAR data. We employ the QvdW formalism in this paper because it is the simplest and straightforward way to include the nuclear matter physics into the hadronic equation of state.

II. MODEL

Searching for the CP signatures (or, more generally, for any notable deviations from the Poisson baseline) within an equilibrium HRG model is only possible if appropriate hadron-hadron interactions are taken into account. Following [39] we assume that the pressure of the QvdW-HRG system can be written as the sum of three terms:

$$p(T, \mu) = p_M(T, \mu) + p_B(T, \mu) + p_{\bar{B}}(T, \mu), \quad (1)$$

where partial pressures of mesons, baryons, and antibaryons are given by

$$p_M(T, \mu) = \sum_{j \in M} p_j^{id}(T, \mu_j), \quad (2)$$

$$p_{B(\bar{B})}(T, \mu) = \sum_{j \in B(\bar{B})} p_j^{id}(T, \mu_j^{B(\bar{B})}) - an_{B(\bar{B})}^2. \quad (3)$$

Here, p_j^{id} are the ideal Bose-Einstein [Eq. (2)] or Fermi-Dirac [Eq. (3)] pressures, $\mu = (\mu_B, \mu_S, \mu_Q)$ are the chemical

potentials which regulate the average values of the total baryonic number B , strangeness S , and electric charge Q . In Eqs. (2), (3), $\mu_j = b_j \mu_B + s_j \mu_S + q_j \mu_Q$ and

$$\mu_j^{B*} = \mu_j - b p_B - a b n_B^2 + 2 a n_B, \quad (4)$$

$$n_B = \sum_{j \in B} n_j = (1 - b n_B) \sum_{j \in B} n_j^{id}(T, \mu_j^{B*}) \quad (5)$$

are, respectively, the shifted chemical potentials for different baryons and total density of all baryons. Note that Eq. (3) implicitly contains terms of arbitrary large powers of $n_{B(\bar{B})}$, through the transcendental equations (4) and (5). The expressions for μ_j^{B*} and $n_{\bar{B}}$ for the antibaryons are analogous to Eqs. (4) and (5). The net baryonic density is $\rho_B = n_B - n_{\bar{B}}$. The QvdW interactions are assumed to exist between all pairs of baryons and between all pairs of antibaryons, including all the strange (anti)baryons, with the same parameters as for nucleons, $a = 329 \text{ MeV fm}^3$ and $b = 3.42 \text{ fm}^3$ [39]. These a and b parameters were obtained in Ref. [37] by fitting the saturation density, $n_0 = 0.16 \text{ fm}^{-3}$, and binding energy, $E/A = -16 \text{ MeV}$, of the ground state of nuclear matter. Baryon-antibaryon, meson-meson, and meson-(anti)baryon QvdW interactions are neglected. Thus, the present version of the QvdW-HRG model is a “minimal interaction” extension of the IHRG model. It should be noted that the vdW parameters a and b may attain different values in the meson-dominated region of the phase diagram at small μ_B/T and high T (see, e.g., the recent analysis of the lattice data [42]). As our focus here is on the effects of the nuclear liquid-gas criticality in the baryon-rich region, we retain the a and b parameter values found from nuclear ground state properties. For the same reason we omit the possible vdW-like interactions between baryons and antibaryons. Since we do not study strangeness related observables, we do not consider also the possible inclusion of the uncharted strange baryons suggested in [43]. The sums in Eqs. (2) and (3) include all stable hadrons and resonances listed in the Particle Data Tables [44].

The QvdW-HRG equation of state (1)–(5) leads to the liquid-gas phase transition in the symmetric nuclear matter, with a CP at $T_c \cong 19.7 \text{ MeV}$ and $\mu_B^c \cong 908 \text{ MeV}$ [37], where a singular behavior of baryon number fluctuations appears [38].

To calculate the particle number fluctuations in $A + A$ collisions we adopt the thermodynamic freeze-out parameters, which were obtained in Refs. [45,46] by fitting the particle yields at different collision energies within the HRG model. The following simple functional form of the freeze-out curve was obtained [45]:

$$T = a_1 - a_2 \mu_B^2 - a_3 \mu_B^4, \quad \mu_B = \frac{b_1}{1 + b_2 \sqrt{s_{NN}}} \quad (6)$$

with $a_1 = 0.166 \pm 0.002 \text{ GeV}$, $a_2 = 0.139 \pm 0.016 \text{ GeV}^{-1}$, $a_3 = 0.053 \pm 0.021 \text{ GeV}^{-3}$, $b_1 = 1.308 \pm 0.028 \text{ GeV}$, $b_2 = 0.273 \pm 0.008 \text{ GeV}^{-1}$. A flatter chemical freeze-out curve, with a possibly lower limiting $T \sim 145 \text{ MeV}$ value at $\mu_B = 0$, was also suggested in Refs. [47–50] based on fluctuations of conserved charges. As our focus here is the baryon-rich region, we retain the original parametrization of Ref. [45]. It was obtained by analyzing the hadron yield data at collision

energies as low as at the Schwerionen Synchrotron (i.e., $\mu_B/T \simeq 15$).

The fluctuations of conserved charges can be calculated in the grand canonical ensemble (GCE) from the system pressure by taking the derivatives over the corresponding chemical potentials. The net baryon number fluctuations are given by the following normalized cumulants (susceptibilities) ($n = 1, \dots, 4$):

$$\begin{aligned} \chi_n &= \frac{\partial^n (p/T^4)}{\partial (\mu_B/T)^n} = \frac{\partial^n (p_B/T^4)}{\partial (\mu_B/T)^n} + (-1)^n \frac{\partial^n (p_{\bar{B}}/T^4)}{\partial (\mu_{\bar{B}}/T)^n} \\ &\equiv \chi_n^B + (-1)^n \chi_n^{\bar{B}}, \end{aligned} \quad (7)$$

where $\mu_{\bar{B}} \equiv -\mu_B$ is the baryochemical potential (not to be confused with the shifted chemical potentials μ_j^{B*} which are only auxiliary quantities). The simple presentation of the χ_n , with the χ_n^B and $\chi_n^{\bar{B}}$ cumulants in Eq. (7) is due to the absence of correlations between baryons and antibaryons in the QvdW-HRG model, i.e., the probability distribution $\mathcal{P}(N_B, N_{\bar{B}})$ of the number of baryons and antibaryons is the product $\mathcal{P}(N_B, N_{\bar{B}}) = \mathcal{P}_B(N_B) \mathcal{P}_{\bar{B}}(N_{\bar{B}})$.

In the following, we consider the normalized skewness and kurtosis for the net baryonic number fluctuations. They are defined as the corresponding ratios of cumulants

$$S\sigma = \frac{\chi_3}{\chi_2}, \quad \kappa\sigma^2 = \frac{\chi_4}{\chi_2}. \quad (8)$$

III. RESULTS AND DISCUSSION

The μ_B - T contour plots of $S\sigma$ and $\kappa\sigma^2$, as calculated in the QvdW-HRG model, are depicted in Fig. 1. The IHRG model chemical freeze-out curve (6) from Ref. [45] is depicted in Fig. 1 by the dash-dotted line. At each μ_B - T point, the strangeness and electric charge chemical potentials μ_S and μ_Q are determined in the QvdW-HRG model from the condition of strangeness neutrality, $S = 0$, and fixed electric-to-baryon charge ratio, $Q/B = 0.4$. Figure 1 shows that signals from the nuclear matter CP shine brightly in net baryon $S\sigma$ and $\kappa\sigma^2$ across the whole phase diagram probed by the heavy-ion collision experiments.

The mean values, $\langle N_B \rangle$, and central moments, $m_n^B = \sum_{N_B} (N_B - \langle N_B \rangle)^n \mathcal{P}_B(N_B)$, of the corresponding baryon number distributions may be measured in $A + A$ collisions. From these measured values the cumulants of $\mathcal{P}(N_B)$ distribution are found:

$$\begin{aligned} K_1^B &= \langle N_B \rangle, \quad K_2^B = m_2^B, \quad K_3^B = m_3^B, \\ K_4^B &= m_4^B - 3m_2^B. \end{aligned} \quad (9)$$

Similar expressions hold for antibaryon quantities.

The cumulants K_n are connected to χ_n in Eq. (7) as $K_n = VT^3 \chi_n$, where V is the system volume. Therefore, all ratios of cumulants χ_n , in particular those in Eq. (8), are equal to the corresponding ratios of K_n . The “required acceptance” [27,51,52] for the event-by-event measurements in $A + A$ reactions should then satisfy the following requirements: The GCE can be used if only the accepted phase-space region is a *small* part of the whole system. On the other hand, this region should be *large* enough to capture the relevant physics.

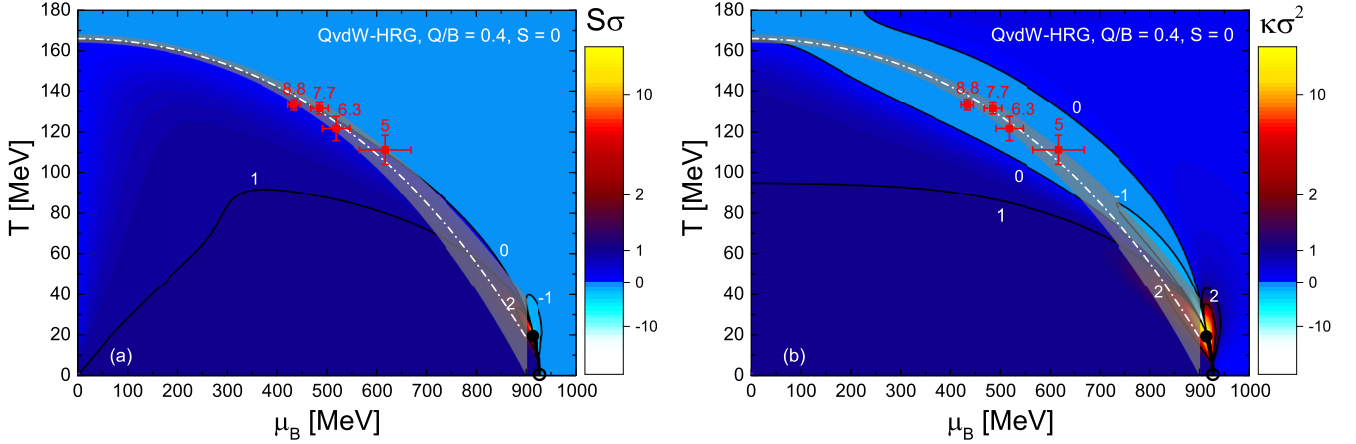


FIG. 1. The contour plots of (a) $S\sigma$ and (b) $\kappa\sigma^2$ for net baryon fluctuations in the μ_B - T plane, as calculated within the QvdW-HRG model. The dash-dotted line shows the IHRG model chemical freeze-out curve [Eq. (6)] from Ref. [45], while the semitransparent shaded area along it depicts the uncertainty in the parameters of this freeze-out curve. The nuclear liquid-gas phase transition is depicted by the thick black line which ends at the CP depicted by full circle. The red circles with error bars correspond to the thermal fits performed within the QvdW-HRG model to the hadron yield data at AGS ($\sqrt{s_{NN}} = 5$ GeV) and SPS ($\sqrt{s_{NN}} = 6.3, 7.7,$ and 8.8 GeV).

Following Refs. [11,27], it is assumed that acceptance corrections from all different sources can be modeled by binomial distributions,

$$P(n) = \sum_{N=n}^{\infty} \mathcal{P}(N) \frac{N!}{n!(N-n)!} q^n (1-q)^{N-n}, \quad (10)$$

where n represents the *measured* number of baryons (or antibaryons), and N represents their *true* numbers. Equation (10) includes the possible effects of isospin randomization, which are also modeled by the binomial distribution [11,53]. The parameter q ($0 \leq q \leq 1$) describes the acceptance effects. In general, it can be different for baryons and antibaryons. Equation (10) gives $P(n) = \mathcal{P}(N)$ for $q = 1$, whereas $P(n)$ becomes the Poisson distribution with $\langle n \rangle = q\langle N \rangle$ in the limit $q \rightarrow 0$. Using Eq. (10), the calculation of all moments and all

cumulants c_n , for all accepted baryons and antibaryons, are straightforward. They are presented as linear combinations, $c_n = a_1 K_1 + \dots + a_n K_n$, with $a_i = a_i(q)$ (see details and explicit expressions in Refs. [11,27]). The STAR data correspond to accepted, efficiency corrected protons and antiprotons at midrapidity ($|y| < 0.5$), in two different transverse momentum intervals: $0.4 < p_T < 0.8$ GeV/c [13] and $0.4 < p_T < 2$ GeV/c [14]. It is further assumed that parameters q for baryons and antibaryons attain the same value. We take $q = 1$ and 0.2 , which approximately represents two cases: (1) the ideal case of all baryons and antibaryons ($q = 1$); (2) a more realistic case of protons and antiprotons within a particular acceptance ($q = 0.2$), including the possible isospin randomization [11,53].

Figure 2 shows the skewness and the kurtosis, as calculated in the QvdW-HRG model, as functions of $\sqrt{s_{NN}}$ along the chemical freeze-out line (6). Solid lines represent the results

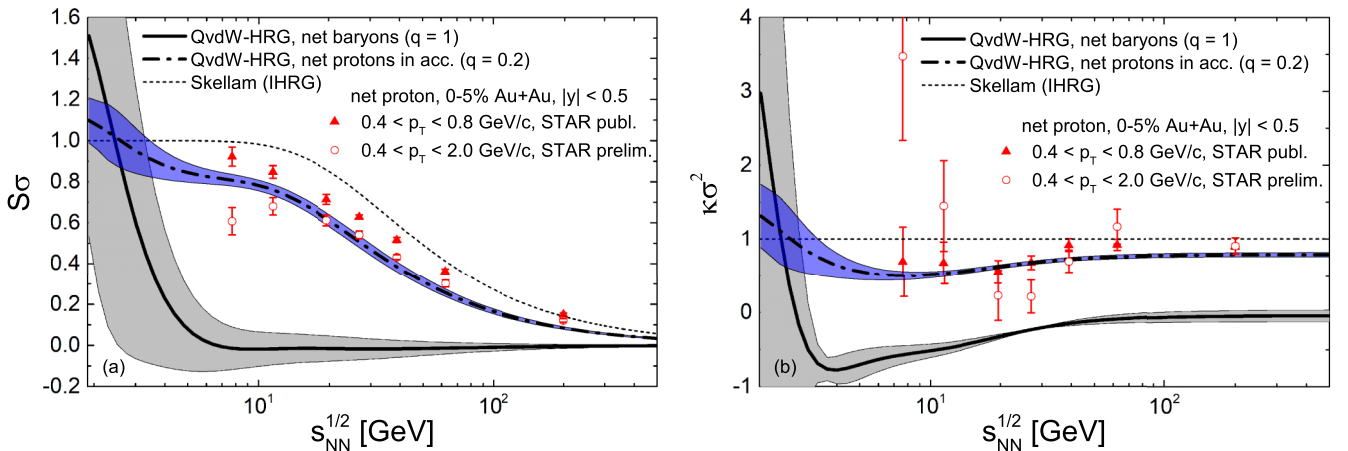


FIG. 2. The (a) $S\sigma$ and (b) $\kappa\sigma^2$ of net baryons in full acceptance (solid lines) and net protons in finite acceptance (dash-dotted lines) as a function of the collision energies in the QvdW-HRG model. The bands estimate the uncertainty coming from the chemical freeze-out curve [Eq. (6)]. The dotted lines correspond to the Skellam distribution baseline of noninteracting hadrons. The STAR collaboration data for the midrapidity net proton fluctuations in the $0.4 < p_T < 0.8$ GeV/c [13] and $0.4 < p_T < 2$ GeV/c [14] intervals are shown by full and open red circles, respectively.

of $S\sigma$ and $\kappa\sigma^2$ of the QvdW-HRG model under the assumption of a full acceptance for both baryons and antibaryons, $q = 1$ in Eq. (10). The kurtosis $\kappa\sigma^2$ shows nonmonotonic behavior at moderate collision energies, similar to the STAR data for net protons [14]. Dash-dotted lines represent the results for $q = 0.2$. Obviously, acceptance effects have a large quantitative and qualitative influence on the behavior of both $S\sigma$ and $\kappa\sigma^2$, and appear to bring them closer to the experimental measurements. Note that the model does not reproduce the preliminary STAR data at the lowest collision energies. This could signal new physics not contained in the purely hadronic QvdW-HRG model, although it may be more prudent to await for these data to be finalized before stronger conclusions can be drawn.

At small q , the QvdW-HRG results approach the baselines obtained from ideal gas calculations, shown in Fig. 2 by the dotted lines. Note that there would be no difference between net baryon and accepted net proton cumulant ratios in the IHRG model. This is because the binomial filter acts as a ‘‘Poissonizer’’, and therefore it does not introduce differences between cumulant ratios of net proton and net baryon distributions in the IHRG model, where fluctuations correspond to Poisson statistics. More detailed IHRG model studies [54] show that net proton fluctuations remain very similar to net baryon fluctuations in the IHRG model even when more effects, such as the probabilistic resonance decays, are taken into account. In contrast to the IHRG model, the presence of baryon-baryon interactions in the QvdW-HRG model makes the net baryon distribution quite different from the Poisson statistics. In this case, the application of the binomial filter changes the cumulant ratios and is the reason for the large difference between the results for net baryon ($q = 1$) and accepted net proton ($q = 0.2$) fluctuation observables seen in Fig. 2.

The binomial filter is only a schematic way to do an acceptance correction, and a more accurate analysis should take into account the correlation range relative to the acceptance. Nevertheless, the binomial filter is fully sufficient to illustrate that the presence of the QvdW interactions between baryons at the chemical freeze-out leads to differences between experimentally observed net proton fluctuations and net baryon fluctuations. This difference can be quite large when baryon-baryon interactions are non-negligible, as suggested by our calculations within the QvdW-HRG model. If the effects of baryonic interactions are indeed significant, then the justification for the direct correspondence between the net baryon cumulant ratios, calculated either from first principles in lattice QCD [55,56] or within effective models for QCD equation of state [57–59], and the net proton cumulant ratios measured in heavy-ion collisions at RHIC, can be questioned. Corrections for differences between net proton and net baryon fluctuations are then required.

We also stress an importance of including the full spectrum of baryonic resonances, which is a new element compared to the earlier works [38,40]. The resonance decay feed-down to the final proton yield could be neglected in the very vicinity of the nuclear liquid-gas transition ($T \lesssim 30$ MeV), but it is essential at the higher temperatures probed by heavy-ion collisions: the resonance decay feed-down accounts for about 10% of all observed protons already at the HADES energy of $\sqrt{s_{NN}} = 2.4$ GeV, and for about 50% of all observed protons at

the lowest STAR-BES energy of $\sqrt{s_{NN}} = 7.7$ GeV. The feed-down from unstable mass fragments can also be important [60]. In the present work we took into account the resonance decay contribution approximately, by applying the binomial filter to all baryons and antibaryons. The full probabilistic decay treatment was considered in Ref. [54] for the IHRG model, a consistent result with binomial filter was reported: no additional significant differences between net proton and net baryon cumulant ratios. It will be interesting to consider the full probabilistic decay treatment in the QvdW-HRG model as well to verify the accuracy of the binomial filter.

One more comment is appropriate here: The chemical freeze-out line (6) used in our studies is determined from the thermal fits to heavy-ion hadron yield data within the simple statistical model for noninteracting hadrons—the IHRG model. This may be approximately valid in the QvdW-HRG model at large collision energies. However, as thermal fits are affected by hadronic interactions [61,62], it is not clear whether a simple IHRG model is appropriate for determination of the chemical freeze-out conditions in the baryon-rich matter created in heavy-ion collisions at $\sqrt{s_{NN}} = 7.7$ GeV and at lower collision energies. As a crosscheck, we have performed thermal fits to the hadron yield data in central heavy ion collisions at the Alternating Gradient Synchrotron (AGS) ($\sqrt{s_{NN}} = 5$ GeV) [63] and Super Proton Synchrotron (SPS) ($\sqrt{s_{NN}} = 6.3, 7.7, \text{ and } 8.8$ GeV) [64] within the chemical equilibrium QvdW-HRG model. The results are depicted in Fig. 2 by the red symbols. This leads to the increased uncertainties of the T and μ_B chemical freeze-out values. Nevertheless, the overall picture is consistent with the chemical freeze-out curve given by Eq. (6). In fact, in the IHRG model itself the chemical freeze-out parameters are also rather uncertain, as illustrated in Fig. 1. Further refinements will be studied in the ongoing and future heavy-ion experiments, such as the HADES experiment [65], the NA61/SHINE experiment [7,66], the STAR fixed-target program [67], the future CBM experiment at FAIR [68], and the future NICA project [69]. The *moderate* collision energies, $\sqrt{s_{NN}} \lesssim 7.7$ GeV, look as the most interesting region for the studies of baryon number fluctuations.

We emphasize that our results give a *qualitative* description of the net proton fluctuations measured at midrapidity in heavy-ion collision experiments. A complete analysis has to take into account other effects including the initial state fluctuations and global charge conservation, as well as possible loss of information about equilibrium fluctuations during the nonequilibrium evolution in the hadronic phase [31]. A dynamical model, incorporating the above effects, and the baryonic interactions, can be used in a *quantitative* study.

IV. SUMMARY

In summary, the QvdW-HRG model, which includes attractive and repulsive vdW interactions between the pairs of baryons and antibaryons, is used to study the higher order cumulants of particle number fluctuations. The cumulant ratios which define the skewness $S\sigma$ and the kurtosis $\kappa\sigma^2$ for baryonic number fluctuations are calculated. These quantities show nonmonotonic structures along the chemical freeze-out

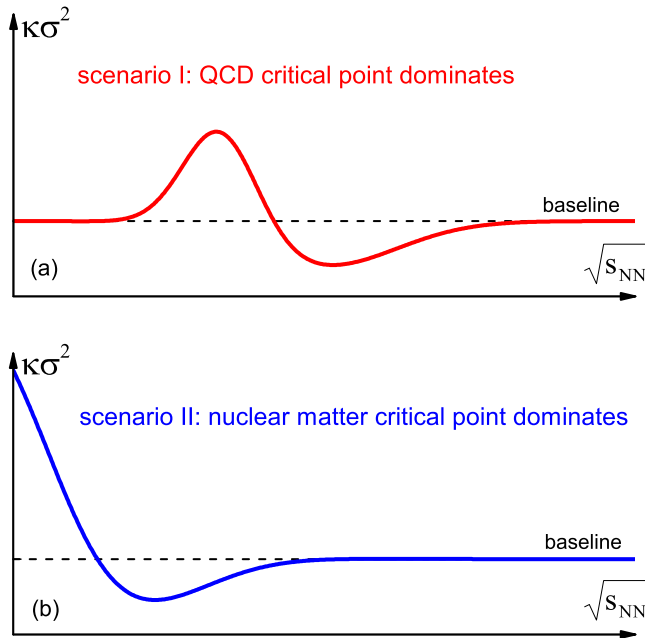


FIG. 3. A schematic view of the collision energy dependence of kurtosis $\kappa\sigma^2$ of net proton fluctuations in two different scenarios. (a) The “standard scenario” [70], where the energy dependence is determined by the chiral CP of QCD. (b) The scenario where the $\kappa\sigma^2$ behavior is determined by the nuclear liquid-gas criticality.

line, which bear similarities to the data presented by the STAR collaboration. These results emphasize the importance of the interactions between baryons for higher order fluctuations. Any serious thermodynamics-based analysis of the net baryon fluctuation measurements should take into account the effects arising from the nuclear liquid-gas criticality.

The QvdW-HRG model predictions for higher-order net baryon fluctuations presented here are quantitatively reliable in the vicinity of the critical point of nuclear matter. A more precise description away from nuclear matter will require refinements and modifications. The present results, however, are sufficient to make an important point regarding the beam energy dependence of the baryon number fluctuations. In the “standard scenario” for the QCD CP, shown in the upper panel of Fig. 3, it is expected that the kurtosis $\kappa\sigma^2$ decreases with decreasing $\sqrt{s_{NN}}$ at moderate collision energies, because the chemical freeze-out (T, μ_B) -point moves away from the hypothetical QCD CP [70]. In contrast, here (lower panel of Fig. 3) $\kappa\sigma^2$ keeps increasing with decreasing $\sqrt{s_{NN}}$, as the chemical freeze-out point moves closer towards the nuclear CP. Future fluctuation measurements and their analysis at moderate collision energies should be able to distinguish these scenarios.

ACKNOWLEDGMENTS

We are grateful to Adam Bzdak, Volker Koch, Misha Stephanov, Jan Steinheimer, and Nu Xu for stimulating discussions. The authors appreciate interesting discussions with the participants at the EMMI Workshop on Critical Fluctuations Near the QCD Phase Boundary in Relativistic Nuclear Collisions, 10–17 October 2017, Wuhan, China. This work was supported by HIC for FAIR within the LOEWE program of the State of Hesse. V.V. acknowledges the support from HGS-HIRe for FAIR. H.St. acknowledges the support through the Judah M. Eisenberg Laureatus Chair at Goethe University. The work of M.I.G. was supported by the Program of Fundamental Research of the Department of Physics and Astronomy of National Academy of Sciences of Ukraine.

- [1] M. A. Stephanov, K. Rajagopal, and E. V. Shuryak, *Phys. Rev. Lett.* **81**, 4816 (1998).
- [2] M. A. Stephanov, K. Rajagopal, and E. V. Shuryak, *Phys. Rev. D* **60**, 114028 (1999).
- [3] M. A. Stephanov, *Prog. Theor. Phys. Suppl.* **153**, 139 (2004); *Int. J. Mod. Phys. A* **20**, 4387 (2005).
- [4] R. A. Lacey *et al.*, *Phys. Rev. Lett.* **98**, 092301 (2007).
- [5] M. M. Aggarwal *et al.* (STAR Collaboration), [arXiv:1007.2613](https://arxiv.org/abs/1007.2613) [nucl-ex].
- [6] X. Luo and N. Xu, *Nucl. Sci. Tech.* **28**, 112 (2017).
- [7] M. Gazdzicki and P. Seyboth, *Acta Phys. Pol. B* **47**, 1201 (2016).
- [8] C. Athanasiou, K. Rajagopal, and M. Stephanov, *Phys. Rev. D* **82**, 074008 (2010).
- [9] Y. Hatta and M. A. Stephanov, *Phys. Rev. Lett.* **91**, 102003 (2003); **91**, 129901(E) (2003).
- [10] M. A. Stephanov, *Phys. Rev. Lett.* **102**, 032301 (2009).
- [11] M. Kitazawa and M. Asakawa, *Phys. Rev. C* **86**, 024904 (2012); **86**, 069902(E) (2012).
- [12] M. M. Aggarwal *et al.* (STAR Collaboration), *Phys. Rev. Lett.* **105**, 022302 (2010).
- [13] L. Adamczyk *et al.* (STAR Collaboration), *Phys. Rev. Lett.* **112**, 032302 (2014).
- [14] X. Luo (STAR Collaboration), *PoS CPOD* **2014**, 019 (2015).
- [15] L. Jiang, P. Li, and H. Song, *Phys. Rev. C* **94**, 024918 (2016).
- [16] B. Ling and M. A. Stephanov, *Phys. Rev. C* **93**, 034915 (2016).
- [17] S. Mukherjee, R. Venugopalan, and Y. Yin, *Phys. Rev. C* **92**, 034912 (2015).
- [18] S. Mukherjee, R. Venugopalan, and Y. Yin, *Phys. Rev. Lett.* **117**, 222301 (2016).
- [19] C. Herold, M. Nahrgang, Y. Yan, and C. Kobdaj, *Phys. Rev. C* **93**, 021902(R) (2016).
- [20] M. Bluhm, M. Nahrgang, S. A. Bass, and T. Schaefer, *Eur. Phys. J. C* **77**, 210 (2017).
- [21] L. Jiang, S. Wu, and H. Song, *Nucl. Phys. A* **967**, 441 (2017).
- [22] J. I. Kapusta, B. Muller, and M. Stephanov, *Phys. Rev. C* **85**, 054906 (2012).
- [23] M. I. Gorenstein and M. Gazdzicki, *Phys. Rev. C* **84**, 014904 (2011).
- [24] E. Sangaline, [arXiv:1505.00261](https://arxiv.org/abs/1505.00261) [nucl-th].
- [25] H. J. Xu, *Phys. Lett. B* **765**, 188 (2017).
- [26] A. Bzdak, V. Koch, and V. Skokov, *Eur. Phys. J. C* **77**, 288 (2017).
- [27] A. Bzdak and V. Koch, *Phys. Rev. C* **86**, 044904 (2012).
- [28] P. Braun-Munzinger, A. Rustamov, and J. Stachel, *Nucl. Phys. A* **960**, 114 (2017).

- [29] V. V. Begun, M. Gazdzicki, M. I. Gorenstein, and O. S. Zozulya, *Phys. Rev. C* **70**, 034901 (2004).
- [30] A. Bzdak, V. Koch, and V. Skokov, *Phys. Rev. C* **87**, 014901 (2013).
- [31] J. Steinheimer, V. Vovchenko, J. Aichelin, M. Bleicher, and H. Stöcker, *Phys. Lett. B* **776**, 32 (2018).
- [32] J. Xu, S. Yu, F. Liu, and X. Luo, *Phys. Rev. C* **94**, 024901 (2016).
- [33] S. He, X. Luo, Y. Nara, S. Esumi, and N. Xu, *Phys. Lett. B* **762**, 296 (2016).
- [34] S. He and X. Luo, *Phys. Lett. B* **774**, 623 (2017).
- [35] A. Bzdak, V. Koch, and N. Strodthoff, *Phys. Rev. C* **95**, 054906 (2017).
- [36] V. Vovchenko, D. V. Anchishkin, and M. I. Gorenstein, *J. Phys. A* **48**, 305001 (2015).
- [37] V. Vovchenko, D. V. Anchishkin, and M. I. Gorenstein, *Phys. Rev. C* **91**, 064314 (2015).
- [38] V. Vovchenko, D. V. Anchishkin, M. I. Gorenstein, and R. V. Poberezhnyuk, *Phys. Rev. C* **92**, 054901 (2015).
- [39] V. Vovchenko, M. I. Gorenstein, and H. Stoecker, *Phys. Rev. Lett.* **118**, 182301 (2017).
- [40] K. Fukushima, *Phys. Rev. C* **91**, 044910 (2015).
- [41] A. Mukherjee, J. Steinheimer, and S. Schramm, *Phys. Rev. C* **96**, 025205 (2017).
- [42] V. Vovchenko, A. Motornenko, M. I. Gorenstein, and H. Stoecker, *Phys. Rev. C* **97**, 035202 (2018).
- [43] P. Alba *et al.*, *Phys. Rev. D* **96**, 034517 (2017).
- [44] C. Patrignani *et al.* (Particle Data Group), *Chin. Phys. C* **40**, 100001 (2016).
- [45] J. Cleymans, H. Oeschler, K. Redlich, and S. Wheaton, *Phys. Rev. C* **73**, 034905 (2006).
- [46] A. Andronic, P. Braun-Munzinger, and J. Stachel, *Nucl. Phys. A* **772**, 167 (2006).
- [47] V. Vovchenko, V. V. Begun, and M. I. Gorenstein, *Phys. Rev. C* **93**, 064906 (2016).
- [48] P. Alba, W. Alberico, R. Bellwied, M. Bluhm, V. Mantovani Sarti, M. Nahrgang, and C. Ratti, *Phys. Lett. B* **738**, 305 (2014).
- [49] A. Bazavov *et al.*, *Phys. Rev. D* **95**, 054504 (2017).
- [50] R. Critelli, J. Noronha, J. Noronha-Hostler, I. Portillo, C. Ratti, and R. Rougemont, *Phys. Rev. D* **96**, 096026 (2017).
- [51] S. Jeon and V. Koch, *Phys. Rev. Lett.* **85**, 2076 (2000).
- [52] M. Asakawa, U. W. Heinz, and B. Muller, *Phys. Rev. Lett.* **85**, 2072 (2000).
- [53] M. Kitazawa and M. Asakawa, *Phys. Rev. C* **85**, 021901(R) (2012).
- [54] M. Nahrgang, M. Bluhm, P. Alba, R. Bellwied, and C. Ratti, *Eur. Phys. J. C* **75**, 573 (2015).
- [55] S. Borsanyi, Z. Fodor, S. D. Katz, S. Krieg, C. Ratti, and K. K. Szabo, *Phys. Rev. Lett.* **113**, 052301 (2014).
- [56] A. Bazavov *et al.* (HotQCD Collaboration), *Phys. Rev. D* **96**, 074510 (2017).
- [57] M. Albright, J. Kapusta, and C. Young, *Phys. Rev. C* **92**, 044904 (2015).
- [58] W. J. Fu, J. M. Pawlowski, F. Rennecke, and B. J. Schaefer, *Phys. Rev. D* **94**, 116020 (2016).
- [59] G. A. Almasi, B. Friman, and K. Redlich, *Phys. Rev. D* **96**, 014027 (2017).
- [60] D. Hahn and H. Stoecker, *Nucl. Phys. A* **476**, 718 (1988).
- [61] V. Vovchenko and H. Stoecker, *J. Phys. G* **44**, 055103 (2017).
- [62] V. Vovchenko and H. Stoecker, *Phys. Rev. C* **95**, 044904 (2017).
- [63] L. Ahle *et al.* (E-802 Collaboration), *Phys. Rev. C* **59**, 2173 (1991); L. Ahle, *ibid.* **60**, 044904 (1999); **60**, 064901 (1999); S. Ahmad *et al.*, *Phys. Lett. B* **382**, 35 (1996); S. Albergo *et al.*, *Phys. Rev. Lett.* **88**, 062301 (2002).
- [64] S. V. Afanasiev *et al.* (NA49 Collaboration), *Phys. Rev. C* **66**, 054902 (2002); C. Alt *et al.* (NA49 Collaboration), *ibid.* **73**, 044910 (2006); **77**, 024903 (2008); **78**, 034918 (2008); **78**, 044907 (2008); *Phys. Rev. Lett.* **94**, 192301 (2005); T. Anticic *et al.*, *Phys. Rev. C* **85**, 044913 (2012); V. Friese, *Nucl. Phys. A* **698**, 487 (2002); see also [<https://edms.cern.ch/document/1075059/4>].
- [65] G. Agakichiev *et al.* (HADES Collaboration), *Eur. Phys. J. A* **41**, 243 (2009).
- [66] N. Abgrall *et al.* (NA61 Collaboration), *JINST* **9**, P06005 (2014).
- [67] K. C. Meehan (STAR Collaboration), *J. Phys. Conf. Ser.* **742**, 012022 (2016).
- [68] T. Ablyazimov *et al.* (CBM Collaboration), *Eur. Phys. J. A* **53**, 60 (2017).
- [69] V. Kekelidze, A. Kovalenko, R. Lednicky, V. Matveev, I. Meshkov, A. Sorin, and G. Trubnikov, *Nucl. Phys. A* **956**, 846 (2016).
- [70] M. A. Stephanov, *J. Phys. G* **38**, 124147 (2011).